Histol Histopathol (2006) 21: 487-501

http://www.hh.um.es

Histology and Histopathology

Cellular and Molecular Biology

Naris occlusion alters transductory protein immunoreactivity in olfactory epithelium

D.M. Coppola[1], A.M. Waguespack[2], M.R. Reems[3], M.L. Butman[4] and J.A. Cherry[4]

[1]Department of Biology, Randolph-Macon College, Ashland, VA, [2]Neuroscience Program, Centenary College, Shreveport, USA, [3]Clinical Science, College of Veterinary Medicine, Colorado State University, Fort Collins, USA and [4]Department of Psychology, Boston University, Boston , USA

Summary. We have recently shown that unilateral naris occlusion (UNO) causes an increase in olfactory marker protein (OMP) immunoreactivity (IR) in mouse olfactory sensory neurons (OSN) from the occluded side of the nasal cavity and a decrease in OMP-IR on the non-occluded side, relative to controls. Given OMP's demonstrated role in olfactory modulation, these OMP-IR changes have been interpreted as a compensatory response by OSNs to odor deprivation on the occluded side and to supernormal exposure to odor on the non-occluded side of the nasal cavity. In the current study, we examined the developmental timing and the regional distribution of this process throughout the nasal cavity using immunocytochemistry. Results demonstrate that OMP-IR diverges in OSNs from the occluded side relative to the non-occluded side of the nasal cavity within eleven days after UNO, with statistically significant differences measurable after 17 days (n=16). We also measured relative levels of the Type 4 phosphodiesterase (PDE4A), another potential olfactory modulator, in nasal cavity tissue from UNO (n=8) and untreated mice (n=9) using western blots and immunocytochemistry. Like OMP, PDE4A-IR increased on the occluded side of the nasal cavity after UNO. Finally, we used immunocytochemistry to assess relative levels of olfactory-specific adenylyl cyclase (AC_{III}, n=4) and G-protein (G_{olf}, n=2) in OSNs from the occluded and non-occluded sides of the nasal cavity of UNO mice. Following UNO, AC_{III} but not G_{olf} -IR levels diverged comparing the occluded to the non-occluded sides of the nasal cavity. Taken together, our findings provide support for the previously unknown phenomenon of compensatory responses by OSNs to odor environment.

Key words: Naris occlusion, Olfactory epithelium, Olfactory marker protein, Phosphodiesterase, Adenylyl cyclase

Offprint request to: Dr David Coppola, Department of Biology, Copley Science Center, Randolph-Macon College, 304 Caroline St., Ashland VA 23005, USA. e-mail: dcoppola@rmc.edu

Introduction

In the olfactory system, most of what is known about the role of neural activity in development comes from studies using unilateral naris occlusion (UNO) as the method of sensory deprivation. In this procedure, one naris is surgically occluded, a technique first performed by Meisami (1976). Though UNO does not result in absolute olfactory deprivation (Coppola et al., 1994), it produces a variety of effects in the ipsilateral olfactory bulb within days or weeks after occlusion, including reduction in bulb volume (Mesiami and Safari, 1981; Frazier and Brunjes, 1988; Brunjes, 1994), reduction in the number of interneurons (Frazier and Brunjes, 1988) and a variety of alterations in the chemistry and physiology of the bulb (e.g. Meisami and Mousavi, 1982; Brunjes, 1985; Baker, 1990; Guthrie et al., 1990). The effects of olfactory deprivation have a sensitive period, a fact consonant with the phenomena of deprivation in other sensory systems. In rodents, where this has been studied in detail, the sensitive period extends through the first few weeks of life (reviewed by Brunjes, 1994). Recent molecular studies suggest that neural activity and competition between afferents, important players in visual development, may be determinants of olfactory receptor survival (Zhao and Reed, 2001; Zou et al, 2004).

Studies of the effects of UNO, like the case with visual and auditory deprivation, have tended to focus on central sequelae. Thus relatively little is known about the effect of UNO on olfactory mucosa. In the mouse, rat, and rabbit, UNO results in a decrease in the thickness of the respiratory and glandular layers of the nasal mucosa as well as the olfactory receptor epithelium (Farbman et al., 1988; Stahl et al., 1990). In the rat, a decline in the rate of mitosis after UNO occurs both in respiratory and olfactory receptor epithelium (Farbman et al., 1988). Recently, we have shown that OMP, a protein implicated in OSN modulation, increases in concentration on the occluded side of the nasal cavity of UNO mice compared to untreated mice (Waguespack et al., 2005).

Conversely, we have shown that OMP decreases in concentration in olfactory receptor cells on the non-occluded side of the nasal cavity of UNO mice (ibid). Since neurons on the occluded side of the nasal cavity are largely deprived of odor exposure while neurons on the non-occluded side experience greater airflow and thus greater odor exposure than normal, OMP concentration changes resulting from UNO appear to have an inverse relationship to odor exposure. Our interpretation of these results is that, given OMP's suspected involvement in olfactory transduction/modulation, its concentration change with odor exposure might be part of a compensatory response by OSNs to different odor environments (Waguespack et al., 2005). Here we extend our work on changes in OSN transduction/modulation pathways following naris occlusion by asking: 1) How soon after naris occlusion can a difference in olfactory receptor cell OMP concentration be detected by immunocytochemisty (ICC)? We reasoned that the latency of response may provide clues as to the underlying mechanism of this phenomenon. 2) Are changes in OMP-IR following UNO uniform across the olfactory mucosa or are they concentrated rostrally as is the case with some long-term pathological effects of UNO on the non-occluded side of the nasal cavity? This question addresses whether we are studying a phenomenon similar to or different from previously described pathological effects. And, 3) are concentrations of PDE4A, Golf, and ACIII, proteins known or suspected to be involved in olfactory transduction/modulation, influenced by UNO, as would be expected under our compensatory hypothesis? By posing the last question, we sought logical extensions of our compensatory hypothesis to proteins that have well understood roles in olfactory transduction, or in the case of PDE4A, to proteins that are believe to be involved in olfactory modulation. Our results provide further support for the idea that olfactory neurons up and down regulate transductory/modulatory proteins in response to odor exposure history.

Materials and methods

Animals

Animal care and experimental procedures on CD-1 strain mice (Charles River Labs Wilmington, MA) followed the Guide to the Care and Use of Laboratory Animals (National Institutes of Health, USA) and were approved by the Randolph-Macon College Institutional Animal Care and Use Committee.

Naris Occlusion

On the day after birth (PND 1), anesthetized (Ketamine & hypothermia) mice had either their left or right naris occluded by cautery. Since left naris occlusions were much easier for a right-handed investigator, and since there was no reasons to believe that side mattered, most animals received left naris occlusion. Several previous studies (see references in introduction) have established that sham cauterization of the snout without actual occlusion has no detectable effect on the olfactory epithelium or olfactory bulbs and so shams were not included in this study.

Every other day after naris occlusion the cauterized naris was inspected to insure it remained occluded. Animals were excluded from the study if their cauterized naris became patent.

Immunocytochemsitry

On PND 6, 12, 18 or 24, mice were deeply anesthetized (Nembutal), exsanguinated with 0.1M PBS (pH 7.2) perfusion, and fixed by perfusion with Bouin's fluid. Trimmed heads were postfixed for 2 hours in Bouin's, and dehydrated in a graded series of ethanol. Heads were then cleared in Histosol, (National Diagnostics, Atlanta, GA), embedded in paraffin, and cut at 10 μm in the coronal plane.

Sections were mounted on subbed microscope slides and reacted for 24 hrs at 4°C with goat anti-OMP (1:30,000; gift of Frank Margolis), rabbit polyclonal antibodies that recognize G_{olf}, AC_{III} (1:300 to 1:2000; Sant Cruz Biotechnology, CA) or a rabbit polyclonal antibody to PDE4A (1:200 Cherry and Davis, 1995). Alternate sections through the olfactory mucosa were stained with Hemotoxylin and Eosin. For selected animals, extracted olfactory bulbs were cut at 20 mm in the horizontal plane on a cryostat followed by staining for Nissl substance. A smaller olfactory bulb, with reduction in thickness of each bulb layer, was taken as evidence of successful naris occlusion (Brunjes, 1985).

Immunoreactivity was visualized using an ABC kit matched to the source of the primary antibody (Vector Labs, Burlingame, CA) and DAB kit (Vector Labs). Primary antibody was omitted in some assays to establish specificity of staining. Preadsorption controls were preformed by Wei et al. (1998) in olfactory cilia for the G_{olf}, AC_{III} antibodies used in this study.

The fixed nasal cavity of one PND 18 animal that had previously undergone UNO was cut on a cryostat. These cryostat sections were reacted with anti-AC_{III} (1:200) followed by visualization with the fluorescent conjugated rabbit antibody Cy-2 (Jackson Labs, MA) or ABC-DAB procedure (see above).

Where detailed quantification was to be carried out (see below) three sections per animal through the rostrocaudal extent of the olfactory epithelium were selected for analysis: one from the rostral one-third, one from the middle one-third, and one from the caudal one-third of the nasal cavity. A complete section, closest to the middle of each region of the nasal cavity, was selected. Within each rostral section, three areas (ventromedial, dorsal recess, and lateral) of the olfactory epithelium were examined. A fourth area on the turbinates was also measured for the middle and caudal sections.

Quantification of immunocytochemistry

Detailed quantification was carried out only for OMP labeling. Measurements were made in both the left and right olfactory mucosa for four UNO mice of each age group. In addition, OMP labeling was quantified for one untreated mouse at PND 6, 12, 18 and two at PND 24.

Image-J software (NIH, USA) was used to quantify IR by measuring the optical density of OSN cell body images. Slides were coded so that the analysis could be done without knowledge of the treatment conditions. Measurements of twenty cell bodies at each sampling site were made from digital photomicrographs taken at 400X magnification. To eliminate bias, a grid image was used to select olfactory receptor cells for measurement. The grid image was overlaid on top of the histological images for each section. Only olfactory neuron cell bodies that intersected the x and y axes of the grid and contained specific OMP labeling were measured. Cell bodies of selected cells were outlined with the computer cursor using the Image-J software. OSN nuclei, which appeared in the cross sections of some cells, did not contain OMP and thus reduced the overall OD of the cell body. However, since the appearance of nuclei in measured cells was not biased with respect to the treatments of interest, we chose to ignore this random factor. Cell optical densities are reported as % light transmission (greater light transmission corresponds to lesser immunoreactivity). Our quantification procedures were similar to Carr et al. (1998). Briefly, measurements were made on digital micrographs recorded at a microscope light setting that corresponded to the point at which a blank part of the slide measured 100% transmission and an opaque part of the slide measured 0% transmission. No attempt was made to normalize measurements to background immunostaining. Since background appears to be a random factor, unrelated to UNO treatment, our simplified procedure should lead to more conservative inferences.

Western blots

Olfactory tissue homogenates were generated from ten PND 24 untreated mice and ten PND 24 UNO treated mice. However, two of the former samples and one of the latter samples were eventually lost in processing.

Under Nembutal anesthesia, olfactory turbinates from the left and right nasal cavity were rapidly dissected into ice-cold phosphate buffered saline (PBS). Turbinates were coded to allow the remaining procedures to be performed without knowledge of the treatments. Tissues were homogenized in ice-cold phosphate buffer. The protein concentration of each homogenate was determined by Bradford analysis (BioRad, Hercules, CA). Aliquots containing 10 µg of protein were boiled in SDS gel-loading buffer, and loaded onto 7.5% SDS-polyacrylamide gels. Each nasal cavity had its own lane in the gel and each sample was run in two separate gels. Data are reported for one replicate but similar results were found for both. Following electrophoresis, gels were incubated for 24 hrs at 4°C in PDE4A primary antibody (1:1000). This antibody had previously undergone an extensive battery of control procedures including preadsorption controls with the antigen used to make the antibody (Cherry and David, 1999).

PDE4A labeling was visualized with an ABC Elite Kit (Vector Labs) following the manufactures instructions. The replicates mentioned above differed in the length of time they were exposed to substrate in order to produce "lighter" and "darker" bands determined subjectively during development. Only the lighter gels were quantified. Intensity of bands on the gel was analyzed using MultiAnalyst (Bio-Rad Laboratories Inc., Hercules, CA) a dedicated densitometer.

The appropriate antibody concentration to demonstrate differential labeling was determined in preliminary studies (not shown).

The sample size for each experiment can be found in Table 1.

Results

The effect of UNO on the morphology of the mouse olfactory system appears to be quite similar to that reported for the rat (Farbman et al., 1988; reviewed by Brunjes, 1994). Nissl stained horizontal sections through the olfactory bulb of PND 24 mice that had UNO on PND 1 evidenced a marked decrease in the size of the ipsilateral olfactory bulb (Fig. 1a). There was a similar decrease in olfactory mucosal thickness on the occluded side of the nasal cavity (Fig. 1b, c) consistent with previous reports in the rat (Farbman et al., 1988) though this was not studied systematically.

Development of OMP-IR

Our previous work showed that OMP-IR increases in OSNs on the occluded side of the nasal cavity and decreases in OSNs on the non-occluded side after 18 days of UNO (Waguespack et al., 2005). Here we

Table 1. number of mice used with each method and antibody.

		AGES			
Method	Antibody	PND 6	PND 12	PND 18	PND 24
ICC	OMP	n: 4	n: 4	n: 4	n: 4
	PDE4A	n: 1		n: 1	
	AC_{III}			n: 1	n: 4
	G_{olf}			n: 1	n: 2
	Untreated	n: 1	n: 1	n: 1	n: 2
Westerns	PDE4A				n: 8
	Untreated				n: 9

concentrated on the development of the divergence between olfactory neurons on the occluded and non-occluded sides of the nasal cavity rather than trying to document absolute amounts of OMP-IR relative to untreated animals. This obviated the need to compare IR between animals, a process that is fraught with difficulties due to variable background staining. However, we report measurements of OMP-IR in some key untreated animals for comparison.

At a qualitative level, there were no consistent differences in OMP labeling between the non-occluded and occluded sides of the nasal cavity in PND 6 animals (Fig. 2a,b). Though we made no attempt to measure olfactory mucosal thickness, there was no obvious difference comparing non-occluded and occluded sides of the nasal cavity. Many OSNs on both the non-occluded and occluded sides were heavily labeled for olfactory marker protein throughout the cell body and dendrite.

By PND 12, clear differences could be seen in OMP labeling between the non-occluded and occluded sides of the nasal cavity. The olfactory mucosa on the occluded side tended to be thinner than the non-occluded side and it contained fewer but more heavily stained OSNs (Fig. 2c,d).

In PND 18 and PND 24 mice the qualitative differences apparent in PND 12 animals became more pronounced. Compared to the non-occluded side, the occluded side of the nasal cavity appeared to have thinner mucosa and fewer, but more heavily labeled, OSNs (Fig. 2e-h). Interestingly, OMP labeling seemed to concentrate in the cell body of olfactory neurons on the occluded side of the nasal cavity leading to a lightening of labeling near the olfactory surface, an area dominated by OSN dendrites. Thus, it appears that naris occlusion not only influences OMP concentration but also its localization within OSNs.

Our qualitative impressions of the tissue sections were born out by detailed optical density measurements. Figure 3 shows histograms of OSN optical density measurements for representative animals from each age group showing cells from the occluded and non-occluded sides of the nasal cavity separately. These histograms, based on 440 cell measurements each, show that OMP-IR tends to decrease with age, becomes less variable, and, importantly, diverges in OSNs on the occluded and non-occluded sides of the nasal cavity (Fig. 3.e-h). By PND 18 OSNs from the occluded side of the nasal cavity had optical density distributions shifted toward lower light transmission values (heavier OMP-IR) while cells from non-occluded side of the nasal cavity had the opposite change relative to earlier age groups.

In Fig. 4, means and SEMs for OMP-IR measurements are plotted for each age group and treatment condition. This figure, based on over 7,040 measured cells, confirms the increased average light transmission reading (decreased OMP-IR) with age and the divergence of OMP-IR in the population of OSNs on the occluded and non-occluded sides of the nasal cavity. To perform statistical analysis, all the optical density measurements were pooled for a given animal and side of the nasal cavity. An ANOVA of these data confirmed that both age ($F_{3,24}$=14.4; p<0.0001) and side of the nasal cavity ($F_{1,24}$=8.6; p<0.001) were significant factors. Measurements of OMP-IR in OSNs from two normal animals were similar to those for the open side of the nasal cavity of UNO treated mice (Fig. 4). A post hoc test confirms that by PND 24 light transmission measurements are significantly different between occluded and non-occluded sides of the nasal cavity (paired t=2.6; p<0.04). Also, OSNs on the occluded side of the nasal cavity had significantly lower light transmission readings than OSNs from untreated animals (unpaired t=2.45; p<0.02).

On PND 18, when clear differences could be seen in the overall pattern of OMP labeling, mean differences

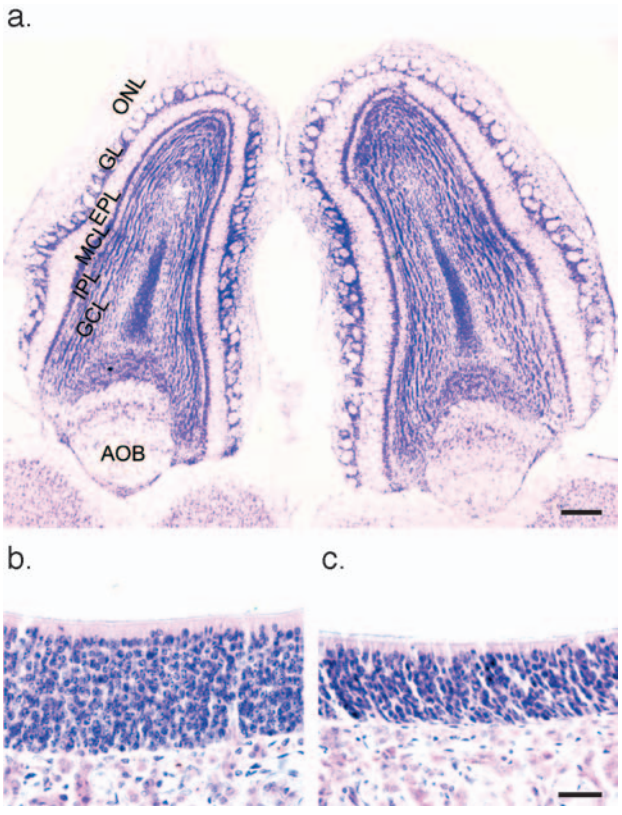

Fig. 1. The effects of UNO at PND 1 on the morphology of olfactory bulbs and mucosa of PND 24 mouse. **a.** Nissl stained horizontal section of olfactory bulbs. Note left bulb, ipsilateral to NO, is approximately 25% smaller than the right bulb. GCL: granule cell layer; IPL: internal plexiform layer; MCL: mitral cell layer; EPL: external plexiform layer; GL: glomerular layer; ONL: olfactory nerve layer. Scale bar: 500 µm. **b.** Hematoxylin and Eosin stained olfactory mucosa section from non-occluded side of the nasal cavity in PND 24 unilaterally naris occluded mouse. **c.** Matching section to B from occluded side of nasal cavity. Note the mucosa is 20 to 30% thinner on the occluded side. Scale bar: 50 µm.

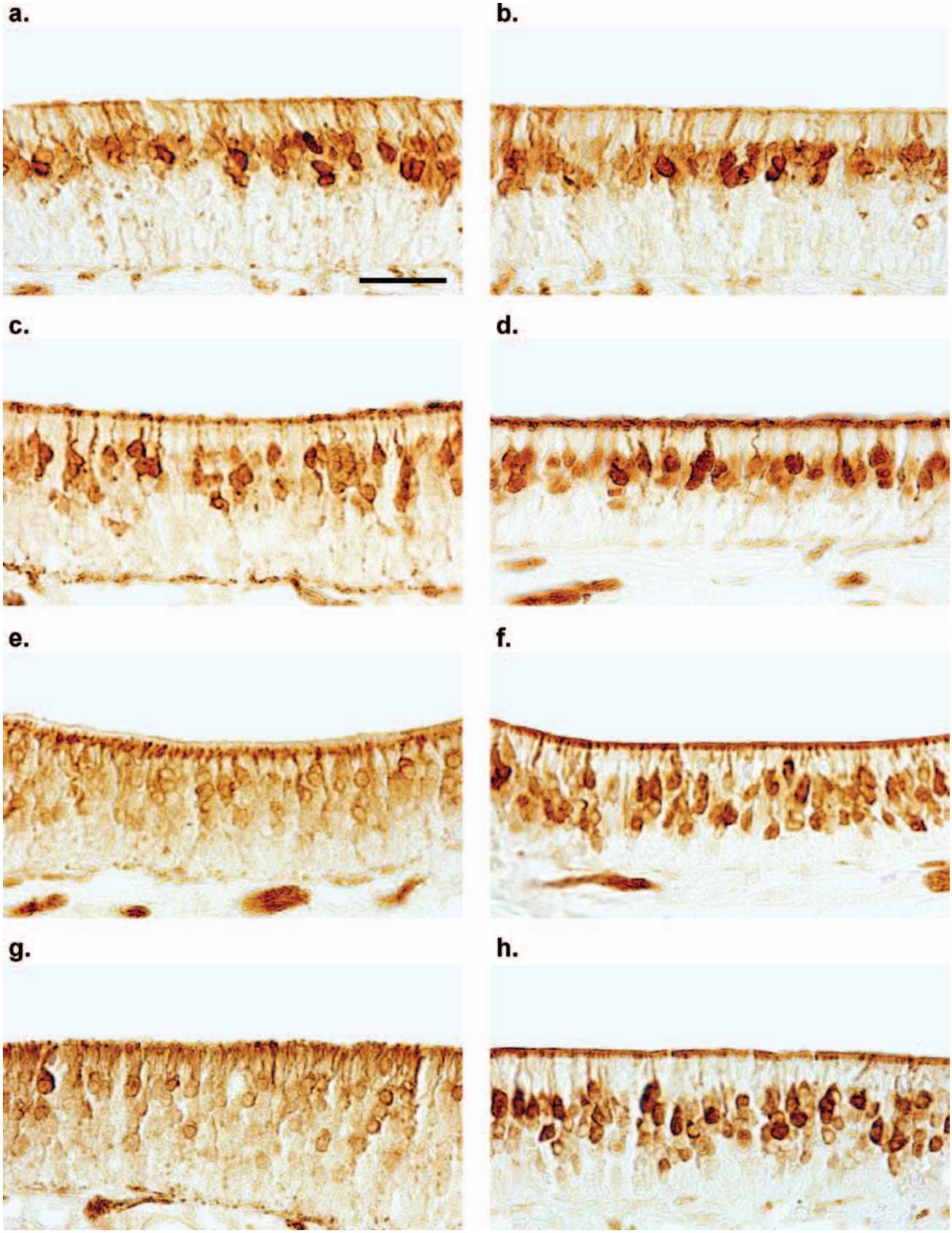

Fig. 2. Photomicrographs of coronal sections from mouse olfactory mucosa labeled with anti-OMP. Each row corresponds to a particular age group as follows: PND 6 **(a, b)**, 12 **(c, d)**, 18 **(e, f)**, and 24 **(g, h)**. The left column **(a, c, e, g)** of photomicrographs is from the non-occluded side of the nasal cavity of UNO animals. Photomicrographs in the right column **(b, d, f, h)** are matched locations from the occluded nasal cavity. Note more dense immunoreactivity in OSNs from the occluded olfactory mucosa (right) at older ages. Divergence of OMP-IR between occluded and non-occluded OSNs is detectable in some PND 12 animals **(d)** but does not become apparent until PND 18 **(f)**. PND 24 **(h)** animals consistently showed the greatest OMP-IR divergence (see text). Scale mark in a: 50 μm.

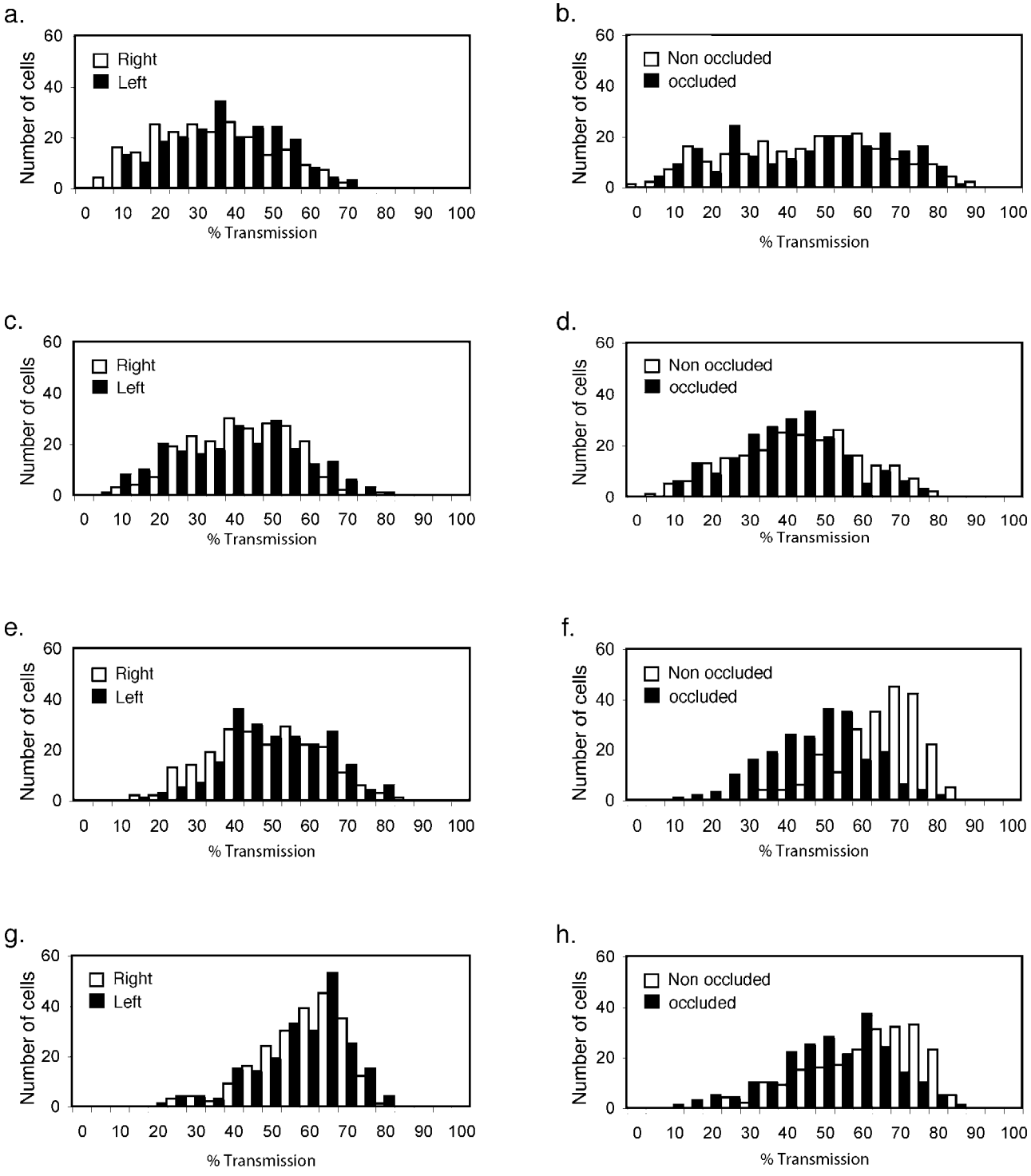

Fig. 3. Histograms of light transmission measurements from OSNs labeled with anti-OMP. Each row of histograms corresponds to a particular age group as follows: PND 6 **(a, b)**, 12 **(c, d)** 18 **(e, f)**), and 24 **(g, h)**. The left column **(a, c, e, g)** of histograms is based on measurements of untreated animals. For these histograms, measurements from the right side of the nasal cavity are compared to the left side. Histograms in the right column **(b, d, f, h)** are based on animals that had undergone UNO on PND1. For these histograms, measurements from the occluded side of the nasal cavity are compared to the non-occluded side. Each histogram is based on 220 OSNs from each side of the nasal cavity in an individual animal. Note divergence of light transmission distribution for occluded versus non-occluded cells at PND18 **(f)** and PND24 **(h)**.

approached but did not reach significance ($p<0.08$). However, the most heavily labeled cells at this age group were clearly found on the occluded side. To test this statistically, we reasoned that under the null hypothesis (no difference in IR between normal and occluded OSNs) the number of cells from the occluded or non-occluded side of the nasal cavity in the lowest percentiles of the joint ranking of light transmission ought to follow a binomial distribution. Thus, we pooled the light transmission values for all 1,760 cells from PND18 mice (four animals pooling left and right nasal cavities) and ranked them. As shown in Fig. 5, olfactory neurons from occluded nasal cavities of PND18 mice were disproportionately represented in the highest 5, 10, and 20% of the joint ranking of optical density (Binomial test; all significant at $p<0.05$ or higher level). Results were similar for rankings of PND24 cells but were not significant for the younger age groups (data not shown).

Regional Comparisons of OMP-IR

Previous work on UNO in mice has established a pathological condition on the non-occluded side of the nasal cavity after long periods (months) of naris occlusion, presumable due to an added respiratory burden (Maruniak et al., 1990). This is particularly pronounced in rostral areas of the olfactory mucosa that experience the greatest airflow. To determine if there were any regional differences in the divergence of OMP-IR on the occluded and non-occluded sides of the nasal cavity, we compared results from rostral, middle, and caudal areas, pooling data from PND18 and PND24 animals. For these age groups, which evidenced the greatest difference in OMP-IR between the occluded and non-occluded sides of the nasal cavity, all three locations in the olfactory mucosa showed a similar tendency for OMP-IR to be more dense in OSNs from the occluded side (Fig. 6). Histograms of light transmission readings from one animal illustrate this general trend (Fig. 7). ANOVA results on the ratio of average light transmission measurements from the occluded and non-occluded sides were not significant comparing across the three locations ($F_{2,20}=0.6$; $p>0.5$). Thus, it appears that the divergence in OMP-IR on the occluded and non-occluded sides of the nasal cavity after UNO occurs to a similar extent in all parts of the nasal cavity.

PDE4A

Having confirmed and extended our earlier result that OMP concentrations diverge in OSNs on the occluded and non-occluded sides of the nasal cavity after UNO, we next wanted to determine if other transductory/modulatory proteins may be similarly effected. PDE4A has a similar localization pattern to OMP except that PDE4A does not occur in the olfactory cilia (Cherry and Davis, 1995). This is not the phosphodiesterase involved in the direct pathway of olfactory transduction, but its high concentration in olfactory receptor cells suggest an important function in some olfactory specific process (Cherry and Davis, 1995).

The results of the western blot analysis reveal an effect of naris occlusion on PDE4A concentration that was similar to that found for OMP (Fig. 8). Lanes containing protein from the occluded side of the nasal cavity tended to have denser PDE4A labeled bands than lanes containing protein from the non-occluded nasal

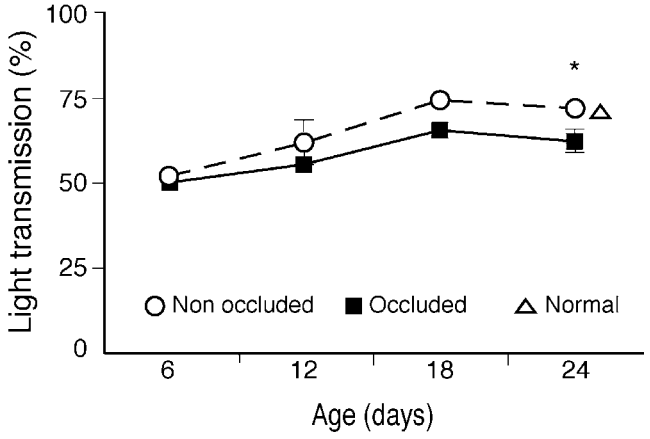

Fig. 4. Averages ± SEMs of pooled light transmission measurements from non-occluded, occluded, or normal (untreated) nasal cavities of mice at different ages (see Table 1). There was a significant increase in light transmission (decrease in OMP-IR) with age for non-occluded and occluded nasal cavities. Note divergence in average light transmission between occluded and non-occluded nasal cavities beginning at PND12 that is statistically significant by PND24 (see text). Normal group at PND 24 is shown for comparison. Where error-bar is not visible it is smaller than symbol diameter. *: $p<0.05$

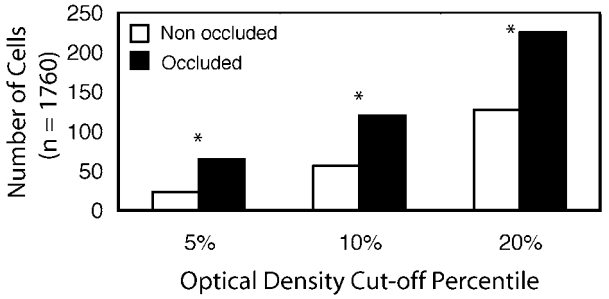

Fig. 5. Tally of cells from four PND18 mice that had undergone UNO at PND1. Shown are the number of OSNs from the non-occluded and occluded sides of the nasal cavity whose optical densities (inverse of light transmission) are in the top 5, 10, and 20% of the joint ranking of all cells. Note significantly more cells from occluded nasal cavities at all three criterion levels, *: $p<0.05$ by Binomial test.

cavity (Fig. 8b; paired t_7=6.6, p<0.001). Also, the optical densities of PDE4A bands from occluded nasal cavities were significantly greater than those from right side nasal cavities of untreated animals (unpaired t_{15}=5.6, p<0.0001). Unexpectedly, there was a significantly greater IR for PDE4A on the right than the left side of the nasal cavity in untreated mice (Fig. 8b; paired t_8=2.7, p<0.05). This curious laterality could not have been the explanation for the differences between the occluded and non-occluded nasal cavities since five out of eight naris occlusions involved the left nasal cavity. Therefore, the confounding factor of laterality likely caused us to

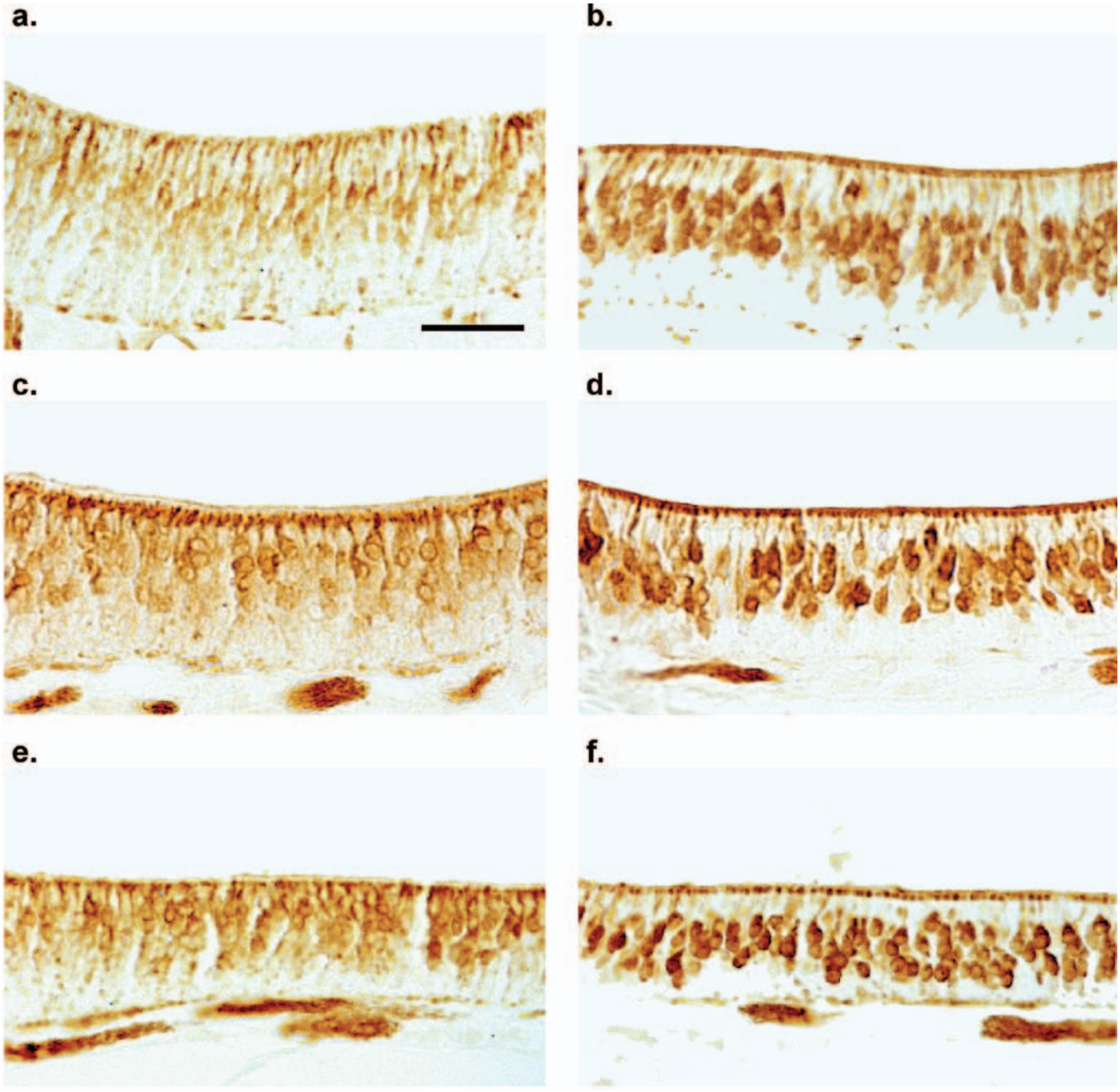

Fig. 6. Photomicrographs of coronal sections labeled with anti-OMP. Representative sections through rostrocaudal extent of the olfactory mucosa of one PND 18 mouse are shown. The animal had undergone UNO on PND 1. Photomicrographs in the left column **(a, c, e)** are from the non-occluded side of the nasal cavity; those in the right column **(b, d, f)** are from the occluded nasal cavity. Top row **(a, b)**: sections from rostral one-third of olfactory mucosa; middle row **(c, d)**: sections from middle one-third of olfactory mucosa; bottom row **(e, f)** sections from the caudal one-third of the olfactory mucosa. Note similar divergence of OMP-IR between occluded and non-occluded OSNs across rostrocaudal locations. Scale bar: 50 μm.

underestimate the difference in IR for PDE4A between occluded and non-occluded sides of the nasal cavity.

Immunocytochemical labeling for PDE4A in one PND6 and one PND18 naris occluded mouse were consistent with western blot results for PND24 mice. Tissue sections from both age groups show denser PDE4A label in OSNs on the occluded side of the nasal cavity compared to the non-occluded side (Fig. 9). As is typical for this antibody, labeling was limited to olfactory receptor cells and their dendrites. Particularly dense labeling was found in dendritic knobs of olfactory receptor cells on the occluded side of the nasal cavity (Fig. 9).

AC_{III} & G_{olf}

G_{olf} is the OSN specific G-protein that links odorant binding to adenylyl cyclase production in the olfactory transductory cascade (reviewed by Ronnett and Moon, 2002). AC_{III} is the form of adenylyl cyclase that catalyzes the production of cAMP, the olfactory second messenger that opens cation channels thus depolarizing OSNs. Previously we have proposed that the observed

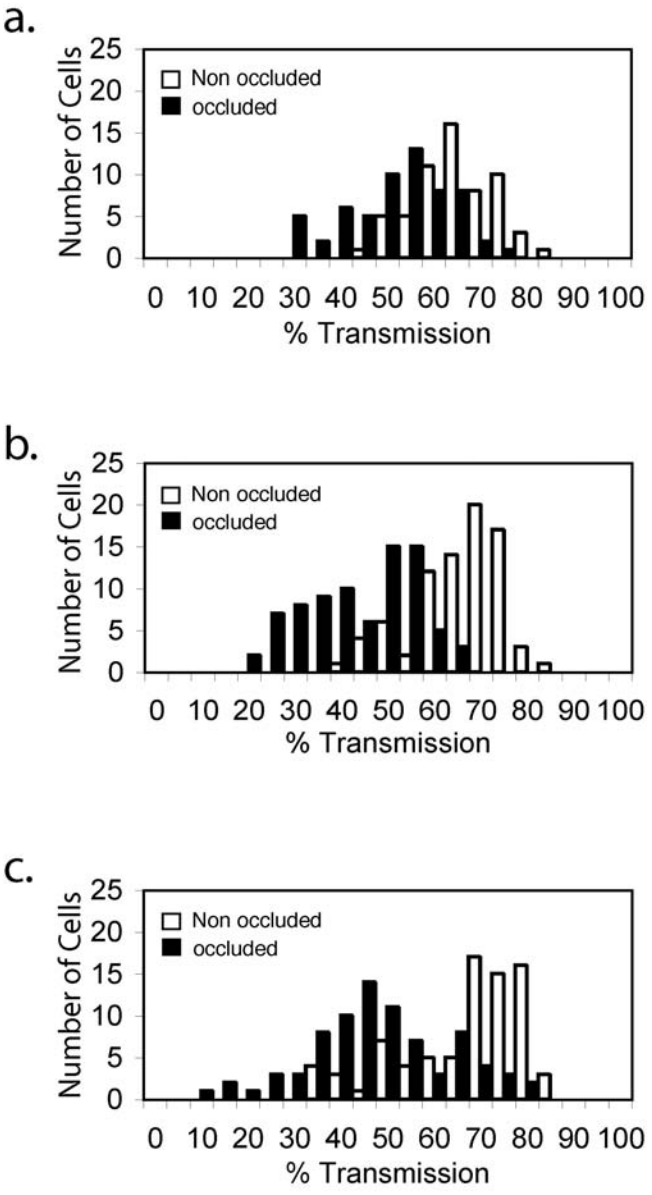

Fig. 7. Histograms of light transmission measurements from OSNs labeled with anti-OMP. Measurements from one PND18 animal that had received UNO on PND1 are shown. Each histogram is based on 120 **(a)** or 160 **(b, c)** cells. **a.** Measurements from rostral one-third of nasal cavity; **b.** Measurements from middle one third of nasal cavity; **c.** Measurements from caudal one-third of nasal cavity. Note similar divergence of OMP-IR across rostrocaudal sampling sites.

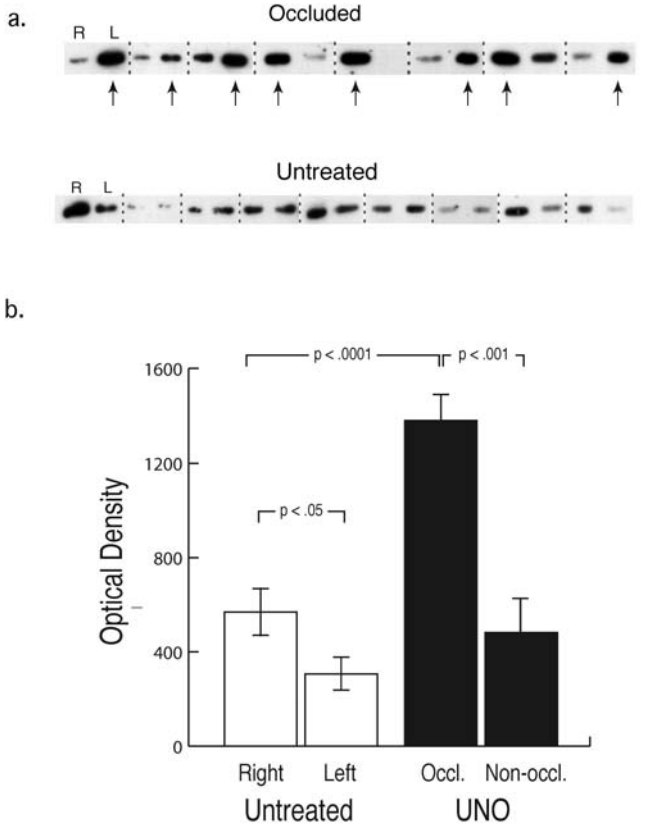

Fig. 8. Western blots of olfactory tissue labeled for PDE4A from left and right sides of the nasal cavity of individual mice. Letters over left-most lane show the orientation of left and right nasal cavity protein across the gel (right and left are reversed in figure). The tissue was collected from PND24 mice that had received UNO on PND1 (top row in **(a)**) or were untreated (bottom row in **(a)**). Arrows under occluded blots designate the occluded side of the nasal cavity. **b.** The mean + SEM optical density for each type of nasal cavity are graphed. Probabilities for within animal comparisons are from paired t-tests; those for between animal comparisons are from unpaired t-test. (see text).

changes in OMP concentration following naris occlusion may represent a compensatory response by OSNs to varying odor environments. In the proposed scheme, chronic exposure to low odor environments would trigger a change in concentration (or activity) of proteins involved in olfactory transduction/modulation so as to make OSNs more sensitive with high odor environments triggering the opposite effect (Waguespack et al., 2005). If odor environment (odor exposure history) causes compensatory responses in OSNs, molecules directly involved in odor transduction, like G_{olf} and AC_{III}, may be affected. To determine if the concentration of these proteins changed following UNO, similar to OMP and PDE4A, we used immunocytochemical labeling in PND18 and PND24 animals.

There was no detectable difference in the amount or pattern of G_{olf} labeling comparing olfactory receptor cells from the occluded and non-occluded sides of the nasal cavity (data not shown). However, there were clear and consistent differences between the occluded and non-occluded sides of the nasal cavity in each of the four animals labeled for AC_{III} (Fig. 10). AC_{III} is localized to olfactory cilia (see Ronnett and Moon, 2002). Therefore, we first had to establish that our labeling pattern was consistent with the known distribution of this enzyme. Both Cy-2 and DAB clearly established very specific labeling at the surface of olfactory, but not respiratory epithelium (Fig. 10a, b). At lower antibody dilutions, denser and more extensive AC_{III} labeling was evident in the olfactory mucosa from the occluded compared to the

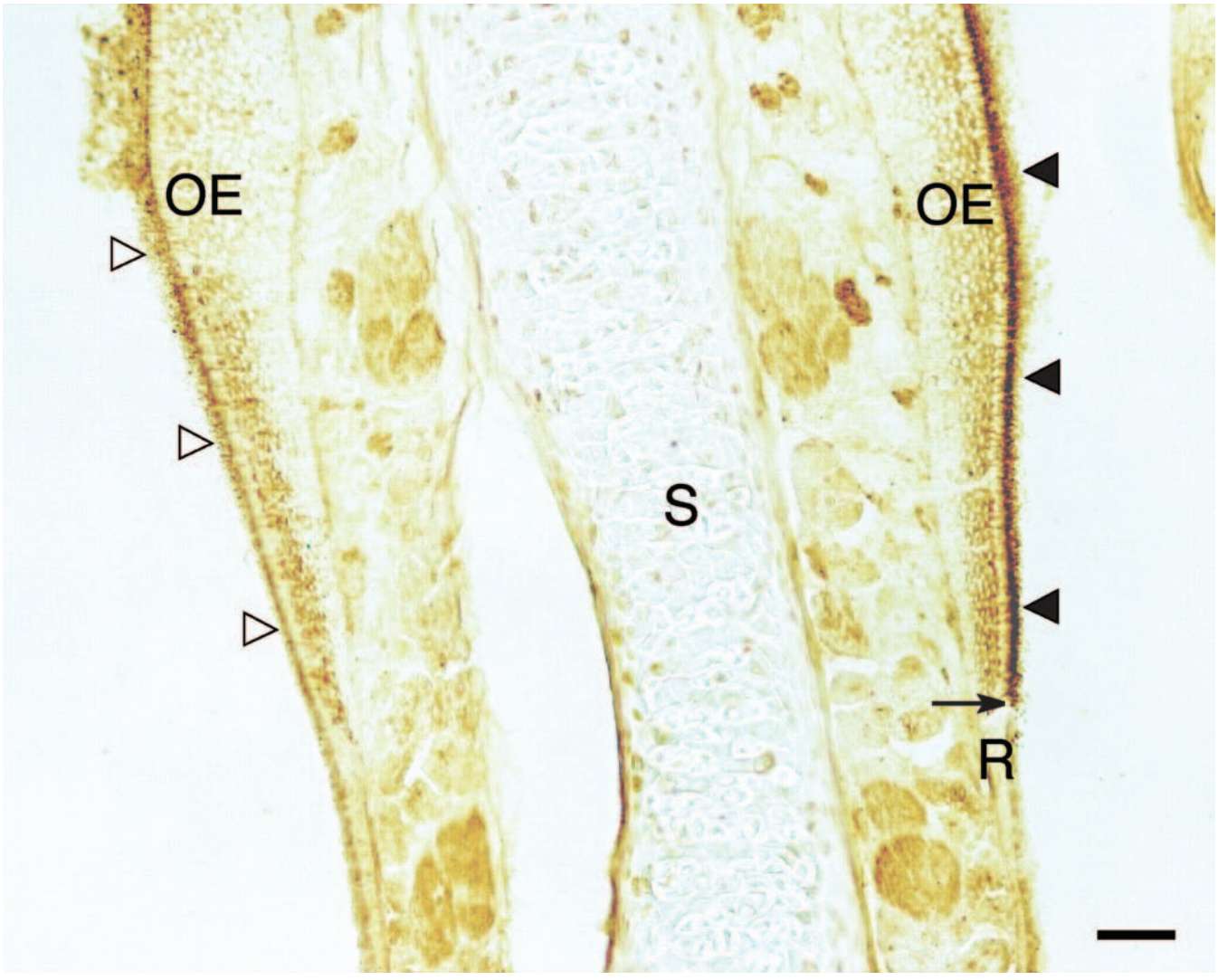

Fig. 9. Coronal section, labeled for PDE4A, of olfactory septum and attached mucosa from PDE18 mouse that had UNO on PND 1. OE: olfactory epithelium; R: respiratory epithelium; S: nasal septum; Filled triangles: occluded side of nasal cavity; Unfilled triangles: non-occluded side of nasal cavity; Arrow: border of R and S. Scale bar: 50 µm.

non-occluded side of the nasal cavity (Fig. 10d, e). Whether this represents an increase compared to normal on the occluded side of the nasal cavity or a decrease on the non-occluded side remains to be investigated.

Discussion

Development and localization of OMP divergence following UNO

OMP is a 19-kD acidic protein that is abundant in the cytosol of mature olfactory neurons of vertebrates (Margolis, 1972; Farbman and Margolis, 1980). Though its exact function remains unknown, recent studies of OMP-null mice establish that this protein is involved in olfactory signal transduction/modulation (Buiakova et al., 1996). OMP-null mutants have a reduced electrophysiological response to single odor stimulation and rapidly repeated stimulation leads to a further diminution of response (Buiakova et al., 1996). Normal function of OSNs in OMP-null mutants can be obtained by adding back OMP coding regions with an adenoviral vector (Ivic et al., 2000). Lastly, odor detection and discrimination behavior are significantly compromised in OMP-null mutant mice (Youngentob and Margolis, 1999; Youngentob et al., 2001), but can be reinstated following adenovirus vector-mediated rescue of OMP in mutant mice (Youngentob et al., 2004).

Our previous work has shown that UNO causes a bidirectional change in OMP-IR, increasing it on the occluded side of the nasal cavity and decreasing it on the non-occluded side (Waguespack et al., 2005). Our goal here was to determine the timing of this divergence in OMP-IR. We found that within 11 days of naris occlusion OMP-IR was already beginning to diverge in OSNs from the occluded and non-occluded sides of the nasal cavity, with denser labeling on the occluded side. By 17 days after naris occlusion the proportion of heavily labeled olfactory receptor was statistically greater on the occluded side of the nasal cavity, a difference that became more pronounced 23 days after UNO. In contrast to our earlier results, the optical density of OMP-IR in olfactory receptor cells from untreated mice was not significantly different from that in olfactory receptor cells from the non-occluded nasal cavity of UNO mice. The failure to fully replicate our earlier results may have been due to the small sample size (n=2) chosen for untreated animals. Comparing

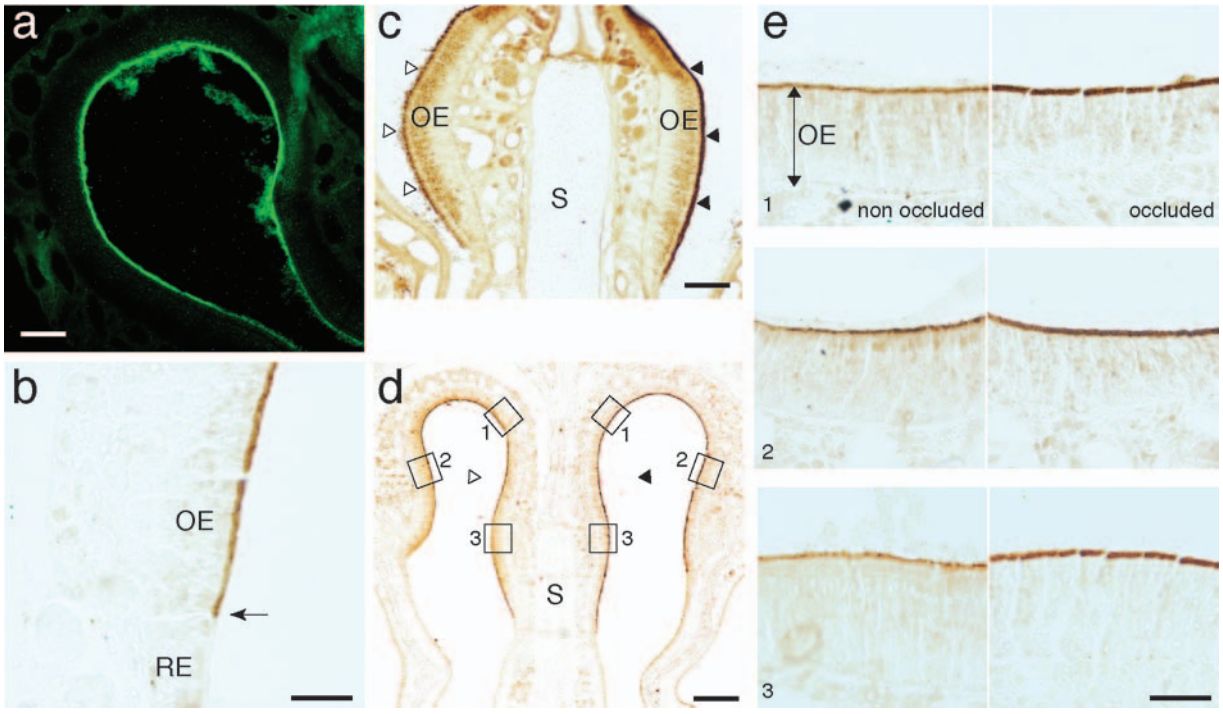

Fig. 10. The effect of UNO at PND1 on AC_{III} labeling in olfactory cilia from one PND 18 and two PND 24 mice. **a.** Cy2 labeling for AC_{III} in non-occluded right nasal cavity shows that label is limited to narrow strip in the region of the olfactory cilia at surface of olfactory mucosa. Scale: 200 µm. **b.** DAB labeling from PND 24 mouse shows the specificity of antibody for olfactory epithelium (OE) at border (arrow) with respiratory epithelium (RE). Scale: 100 µm. **c.** Cryostat section from PND 18 animal that received naris occlusion on PND1. Note heavier IR on occluded (filled triangles) compared to non-occluded (unfilled triangles) side of nasal cavity (s: nasal septum). Scale bar: 200 µm. **d.** Low power photomicrograph of coronal paraffin section from PND 24 mouse (boxes show the approximate location of high power micrographs in e; symbols as above). Scale bar: 400 µm. **e.** High power photomicrographs from areas shown in d. Location 1 and 2 are from the animal shown in d. Location 3 is from a matched location in another animal (other symbols as above). Scale bar: 50 µm. Note AC_{III} labeling is denser and more extensive on the occluded side of the nasal cavity.

untreated and UNO mice involves a comparison between animals rather than within animals and thus is complicated by individual variability in backgrounds labeling. However, on balance, the results from our developmental study are consistent with our previous studies and support the idea of a compensatory response. The fact that it took weeks instead of days to manifest a change in OMP-IR suggests that this process is not part of olfactory adaptation that has a time course of minutes or hours (Munger et al., 2001).

Maruniak and his colleagues (1989, 1990) demonstrated neuron loss and other signs of pathology on the non-occluded side of the nasal cavity in UNO mice that was most pronounced in the rostral part of the olfactory mucosa. These authors speculated that the degradation they observed was due to the unrelenting exposure to toxins, pathogens, and other damaging substances that would be expected at the leading edge of the olfactory mucosa on the non-occluded side of UNO animals (Maruniak et al., 1989, 1990). Based on these findings, we were particularly interested in comparing regions of the nasal cavity for the degree of OMP-IR divergence between sides of the nasal cavity in UNO animals. The differences in OMP-IR between olfactory neurons from the occluded and non-occluded sides of the nasal cavity were consistent across the rostral, middle, and caudal regions. Given the uniformity of the effect and its rapid appearance - apparent within days instead of the several weeks needed before neuron loss was observed in the Maruniak et al. (1989, 1990) studies - we conclude that the OMP changes that we have observed reflect a different phenomenon than that described by these authors.

Thus, the onset of the OMP-IR response to deprivation appears to be too slow to be part of the well-studied phenomenon of olfactory adaptation and too rapid to be part of the previously studied pathological response to deprivation (Maruniak, 1989, 1990; Munger et al., 2001).

A possible explanation for the divergence of OMP-IR on the occluded and non-occluded sides of the nasal cavity in UNO animals emerges from the work of Farbman et al. (1988) who measured the rate of mitosis and counted olfactory knobs on the occluded and non-occluded sides of developing rats that had undergone UNO the day after birth. These authors found that while the rate of mitosis was reduced on the occluded side of the nasal cavity compared to the non-occluded side, the number of mature OSNs was similar on both sides. Thus, it would appear that OSNs, which are known to turn over throughout life in normal animals, might live longer on the occluded side of UNO animals. Since only mature neurons express OMP, it seems possible that differences in OMP-IR in OSNs on the occluded and non-occluded sides of the nasal cavity may be due to differences in OSN birth and death rate in these regions (Monti Graziadei et al., 1977).

However, such a cell dynamic explanation for the divergence of OMP-IR reported in the current study seems unlikely for a number of reasons. First, we only measured neurons in the upper one-third of the olfactory mucosa where one would expect to find mature olfactory neurons. Second, the divergence of OMP-IR between neurons on the occluded and non-occluded sides of the nasal cavity was apparent after 11 days of naris occlusion and was statistically significant by 17 days post occlusion. This is a much briefer period than the life expectancy of OSNs, which has been estimated to be approximately 60 days (Graziadei and Monti Graziadei, 1978). Third, it was rare to find any olfactory neurons on the non-occluded side of the nasal cavity of UNO animals that were as densely labeled for OMP as the average neuron on the occluded side (c.f. Fig. 2 e-h). Even with marked differences in the number of immature neurons, one would expect some older neurons to survive on the non-occluded side. Lastly, we can find no published data to support the premise that the amount of OMP-IR is correlated with the age of OSNs, though it has been established that mature neurons express OMP while immature neurons do not (Monti Graziadei et al., 1977). In fact, on both the occluded and non-occluded sides of the nasal cavity, we found a statistically significant decrease in OMP-IR with age. Collectively, these considerations cast doubt on an explanation of our OMP results based on differences in cell dynamics between olfactory neuron populations on the occluded and non-occluded side of the nasal cavity of UNO animals.

Divergence of PDE4A labeling following UNO

PDE's are part of a large enzyme class with varying specificities and affinities for a variety of cyclic nucleotide substrates (reviewed by Cherry and Davis, 1995). These enzymes are all capable of hydrolyzing 3'-5'-cyclic nucleotides to 5'-monophosphate. Since odorants activate adenylyl cyclase as part of one olfactory transduction pathway, PDE's play a role in controlling the ambient level of cAMP in olfactory receptors (Ronnett and Moon, 2002). Several forms of PDE are expressed in mammalian OSNs and one form, PDE1C2, found only in OSN cilia, may be directly responsible for restoring basal levels of cAMP after odorant stimulation (Borisy et al., 1991, 1993; see review by Ronnet and Moon, 2002). By contrast, Type IV PDEs are abundant in OSN cell bodies and dendrites but are conspicuously absent from OSN cilia (Cherry and Davis, 1995). That PDE4A is involved in olfactory modulation is supported by recent evidence that rolipram, an inhibitor of PDE4A, alters odor detection in mice (Pho et al., 2005). It has been postulated that these enzymes may modulate the parameters of depolarization downstream from the primary signal transduction events in OSNs (Cherry and Davis, 1995).

To study the effect of UNO on PDE4A concentration in OSNs, we concentrated on western blotting for three reasons: 1) the known abundance of PDE4A throughout the cell body and dendrites of olfactory receptor

neurons, 2) the expected reduced variability between animals with this technique relative to immunocytochemistry, and 3) the ease with which we could generate replicates. We used a well-characterized antibody to PDE4A, a Type IV PDE, which labels olfactory receptor cells in a manner similar to OMP (Cherry and Davis, 1995). It was reasoned that the abundance of PDE4A in olfactory receptor cells and its proposed involvement in olfactory modulation made it an interesting comparison to OMP in our paradigm (see Kawai et al., 1999). As with OMP, both our western blots and preliminary immunocytochemistry show significantly denser labeling for PDE4A in OSNs from the occluded side of the nasal cavity relative to the non-occluded side.

An unexpected result from our western blots for PDE4A was the laterality of expression in untreated animals. PDE4A labeling in the western blots of tissue from the right side of the nasal cavity was significantly greater than for the left side. Though not observed in this study, Carr and her coauthors (1998) have noted laterality in OMP staining in untreated rats opposite to what we observed for PDE4A labeling. These authors speculated that laterality in the expression of OMP may be related to an inherent bias in the patency (and thus odor access) of one side of the nasal cavity versus the other. Also, laterality of expression in norepinephrine has been reported in the olfactory bulb of mice (Dluzen and Kreutzberg, 1996).

Unfortunately our poor understanding of non-ciliary PDE function and the significance of its compartmentalization within OSNs make it difficult to speculate further about our result. Nevertheless, the divergence of PDE4A concentration in OSNs from the occluded and non-occluded sides of the nasal cavity are consistent with a compensatory response to odor environment.

G_{olf} and AC_{III}

Though we found that the effects of UNO on OMP and PDE4A expression are phenomenologically similar, the uncertain functions of these two olfactory specific proteins limit the conclusions that can be drawn from these findings alone. In contrast, the role of G_{olf} and AC_{III} in the initial events of olfactory transduction are well established (reviewed by Ronnet and Moon, 2002). As noted previously, G_{olf} links odorant-receptor binding to cAMP production by activating AC_{III}. The second messenger cAMP, in turn, causes cyclic nucleotide gated channels to open triggering a cascade of events, including calcium influx, which depolarizes the OSNs. According to our compensatory hypothesis, OSNs deprived of odorant stimulation, such as those on the occluded side of the nasal cavity of UNO animals, might be expected to up regulate key elements of their transductory pathway so as to increase sensitivity. One potential method of doing this would be to increase the concentration or activity of molecules that link odor-receptor binding to membrane depolarization. This would lead to greater amplification of olfactory signals, presumably at the expense of dynamic range.

Despite the small number of animals used, our results with Golf and ACIII labeling were sufficiently clear and consistent to warrant their inclusion in this report. We found no obvious difference in G_{olf} labeling between OSNs on the occluded and non-occluded sides of the nasal cavity. However, consistent with our hypothesis, AC_{III} labeling was heavier and more extensive in OSNs from the occluded side of the nasal cavity compared to the non-occluded side across the olfactory mucosa and in all four subjects tested. Since the activation of adenylyl cyclase is a key amplification step in G-protein coupled transduction generally, an increase in its concentration in cilia could be expected to profoundly affect the sensitivity of OSNs. Our failure to find a change in Golf after UNO is puzzling unless perhaps AC_{III} concentration has a sufficiently large impact on amplification within the olfactory transduction cascade that changes in Golf are unnecessary. If OSNs are changing their sensitivity or dynamic range in response to chronic changes in odor environment, as we have proposed, it does not follow that every element of the olfactory transduction cascade would be affected.

Long-term plasticity in transductory/modulatory elements within OSNs has received little attention, though densitization and short-term adaptive responses has been studied in detail (Wei et al., 1998; Munger et al., 2001; reviewed by Ronnett and Moon, 2002). Taken together, our results with OMP, PDE4A, and ACIII, point to marked, environmentally-induced, changes in the concentration of proteins that are known or likely modulators of OSN signal transduction. We interpret this as evidence of a previously unknown compensatory response on the part of OSNs to odor environment. Compensatory responses have already been postulated as the explanation for changes in the olfactory bulb following UNO including an increase in dopamine D2 receptors, an increase in norepinephrine receptors, and an enhanced odor induced uptake of 2-deoxyglucose (Leon, 1998). Also, compensatory responses to chronic changes in stimulus level are well known in other sensory systems and among cultured neurons chronically inhibited with drugs (Tian and Copenhagen, 2001; Vale and Sanes, 2002; reviewed by Zhang and Linden, 2003).

An untested assumption upon which the current work and most other studies of olfactory deprivation rest is that the effects of UNO on the olfactory system are exclusively related to stimulus deprivation. Surprisingly, there are few direct tests of this premise owing to the difficulty of depriving animals of odor stimulation by any other means. Yet, occluding the nasal cavity undoubtedly causes many changes in the physiology of the olfactory and non-olfactory tissues. For example, UNO causes an ipsilateral decrease in the rate of mitosis in respiratory as well as olfactory mucosa (Farbman et al., 1988). Therefore, it is possible that some other factor in respired air - eliminated (or at least drastically

reduced) on the occluded side and accentuated on the non-occluded side of UNO animals - explains the results reported here.

Assuming our interpretation is correct, it remains to be seen whether the compensatory phenomenon is limited to the developmental period. As noted above, the effects of UNO on the olfactory bulb have a critical period (reviewed by Brunjes, 1994). We have not studied the effects of UNO on the olfactory mucosa in adults, though it would be interesting to do so. Many other pressing questions remain including: What other transductory elements are involved in the compensatory process? How could the proposed compensatory responses be controlled? And, what physiological effects do the observed changes have on OSNs? Despite these numerous uncertainties, our results shed light on the effect of (partial) sensory deprivation and stimulus enhancement on the olfactory mucosa, a previously understudied process. Our findings also suggest that the rather myopic attention to the deleterious effects of sensory deprivation may have caused us and other previous investigators to miss potentially interesting compensatory responses in the olfactory system.

Acknowledgements. The authors thank Blane Sessions and Dan Epstein for technical assistance. Dr. Frank Margolis kindly donated OMP antibody. Supported by a Research Grant from the National Science Foundation (USA) to DC.

References

Baker H. (1990). Unilateral neonatal olfactory deprivation alters tyrosine hydroxylase expression but not aromatic amino acid decarboxylase or GABA immuoreactivity. Neuroscience 36, 761-771.

Borisy F.F., Hwang P.M., Ronnett G.V. and Snyder S.H. (1993). High affinity cyclic AMP phosphodiesterase and adenosine localized in sensory organs. Brain Res. 610, 199-207.

Borisy F.F., Ronnett G.V., Cunningham A.M., Juilfs D., Beavo J. and Snyder S.H. (1991). Calcium/calmodulin activated phosphodiesterase selectivity expressed in olfactory receptor neurons. J. Neurosci. 12,915-923.

Brunjes P. (1985). Unilateral odor deprivation, time course of changes in laminar volume. Brain Res. Bull. 14, 233- 237.

Brunjes P. (1994). Unilateral naris closure and olfactory system development. Brain Res. Rev. 19, 146-160.

Buiakova O.I., Baker H., Scott J.W., Farbman A., Kream R., Grillo M., Franzen L., Richman M., Davis L.M., Abbondanzo S., Stewart C.L. and Margolis F.L. (1996). Olfactory marker protein (OMP) gene deletion causes altered physiological activity of olfactory sensory neurons. Proc. Natl. Acad. Sci. USA 93, 9858-9863.

Carr V.M., Walters E., Margolis F.L. and Farbman A.I. (1998). An enhanced olfactory marker protein immunoreactivity in individual olfactory receptor neurons following olfactory bulbectomy may relate to increased neurogenesis. J. Neurobiol. 34, 377-390.

Cherry J.A. and Davis R.L. (1995). A mouse homolog of dunce, a gene important for learning and memory in Drosophia, is preferentially expressed in olfactory receptor neurons. J. Neurobiol. 28, 102-113.

Cherry J.A. and Davis R.L. (1999). Cyclic AMP phosphodiesterases are localized in regions of the mouse brain associated with reinforcement, movement, and affect. J. Comp. Neurol. 407, 287-301.

Coppola D.M., Coltrane J.A., and Arsov I. (1994). Retronasal or internasal olfaction can mediate odor-guided behaviors in newborn mice. Physiol. Behav. 56, 729-736.

Dluzen D.E. and Kreutzberg J.D. (1996). Norepinephrine is lateralized within the olfactory bulbs of male mice. J. Neurochem. 66, 1222-1232.

Farbman A.I., Brunjes P.C., Rentfro L., Michas J. and Ritz S. (1988). The effect of unilateral naris occlusion on cell dynamics in the developing rat olfactory epithelium. J. Neurosci. 8, 3290-3295.

Farbman A.I., Buchholz J.A., Walters E. and Margolis F.L. (1998). Does olfactory marker protein participate in olfactory neurogenesis. Ann. NY Acad. Sci. 855, 248-251.

Farbman A.I. and Margolis F.L. (1980). Olfactory marker protein during ontogeny, immunohistochemical localization. Dev. Biol. 74, 205-215.

Frazier L.L. and Brunjes P.C. (1988). Unilateral odor deprivation, early postnatal changes in olfactory bulb cell density and number. J. Comp. Neurol. 269, 355-370.

Graziadei P.P.C. and Monti Graziadei G.A. (1978). Continuous nerve cell renewal in the olfactory system. In: Handbook of sensory physiology. Vol IX. Jacobsen M. (ed). Springer-Verlag. New York. pp. 123-132.

Guthrie K.M., Wilson D.A. and Leon M. (1990). Unilateral olfactory deprivation modifies olfactory bulb function. J. Neurosci. 10, 3402-3412.

Ivic L., Pyrski M.M., Margolis J.W., Richards L.J., Firestein S. and Margolis F.L. (2000). Adenoviral vector-mediated rescue of the OMP-null phenotype in vivo. Nat. Neurosci. 3,1113-1120.

Kawai F., Kurahashi T. and Kaneko A. (1999). Adrenaline enhances odorant contrast by modulating signal encoding in olfactory receptor cells. Nat. Neurosci. 2, 133-138.

Leon M. (1998) Compensatory responses to early olfactory restriction. Ann. NY Acad. Sci. 855, 104-108.

Margolis F.L. (1972). A brain protein unique to the olfactory bulb. Proc. Natl. Acad. Sci. USA 69, 1221-124.

Maruniak J.A., Henegar J.R. and Sweeney T.P. (1990). Effects of long-term unilateral naris closure on the olfactory epithelium of adult mice. Brain Res. 526, 65-72.

Maruniak J.A., Lin P.J. and Henegar J.R. (1989). Effects of unilateral naris closure on the olfactory epithelium of adult mice. Brain Res. 490, 212-218.

Meisami E. (1976). Effects of olfactory deprivation on postnatal growth of the rat olfactory bulb utilizing a new method for production of neonatal unilateral anosmia. Brain Res. 107, 437-444.

Meisami E. and Mousavi R. (1982). Lasting effects of early olfactory deprivation on the growth, DNA, RNA and protein content, and Na-K-ATPase and AChE activity of the rat olfactory bulb. Dev. Brain Res. 2, 217-229.

Meisami V. and Safari L. (1981). A quantitative study of the effects of early unilateral olfactory deprivation on the number and distribution of mitral and tufted cells and of glomeruli in the rat olfactory bulb. Brain Res. 221, 81-107.

Monti Graziadei G.A., Margolis F.L., Harding J.W and Graziadei P.P.C. (1977). Immunocytochemistry of the olfactory marker protein. J. Histochem. Cytochem. 25, 1311-1316.

Munger S.D., Lane A.P., Zhong H., Leinders-Zufall T., Yau K.W., Zufall F. and Reed R.R. (2001). Central role of the CNGA4 channel

subunit in Ca2+-calmodulin-dependent odor adaptation. Science 294, 2172-2175.

Pho V., Butman M.L. and Cherry J.A. (2005). Type 4 phosphodiesterase inhibition impairs detection of low odor concentrations in mice. Behav. Brain Res. 161, 245-253.

Ronnett G.V. and Moon C. (2002). G-protein and olfactory signal transduction. Annu. Rev. Physiol. 64, 189-222.

Stahl B., Distel H. and Hudson R. (1990). Effects of reversible nare occlusion on the development of the olfactory epithelium in the rabbit nasal septum. Cell Tissue Res. 259, 275-281.

Tian N. and Copenhagen D.R. (2001). Visual deprivation alters development of synaptic function in inner retina after eye opening. Neuron 32, 439-449.

Vale C. and Sanes H. (2002). The effect of bilateral deafness on excitatory and inhibitory synaptic strength in the inferior colliculus. Eur. J. Neurosci. 16, 2394-2404.

Waguespack, A.M., Reems M.R., Butman M.L., Cherry J. and Coppola, D.M. (2005). Olfactory receptor neurons have enhanced olfactory marker protein immunoreactivity in the nasal cavity ipsilateral to naris occlusion. Brain Res. 1044, 1-7.

Wei J., Zhao A.Z., Chan G.C.K., Baker L.P., Impey S., Beavo J.A. and Storm D.R. (1998). Phosphorylation and inhibition of olfactory adenylyl cyclase by CaM Kinase II in neurons, a mechanism for attenuation of olfactory signals. Neuron 21, 495-504.

Youngentob S.L. and Margolis F.L. (1999). OMP gene deletion causes an elevation in behavioral threshold sensitivity. Neuroreport 10, 15-19.

Youngentob S.L., Margolis F.L. and Youngentob L.M. (2001). OMP gene deletion results in an alteration in odorant quality perception. Behav. Neurosci 115, 626-631.

Youngentob S.L., Pyrski M.M. and Margolis F.L. (2004). Adenoviral vector-mediated rescue of the OMP-null behavioral phenotype: enhancement of odorant threshold sensitivity. Behav. Neurosci. 118, 636-642.

Zhang W. and Linden D.J. (2003). The other side of the engram, experience-driven changes in neuron intrinsic excitability. Nat. Rev. Neurosci. 4, 885-900.

Zou D., Feinstein P., Rivers A.L., Mathews G.A., Kim A., Greer, C.A., Mombaerts P. and Firestein S. (2004). Postnatal refinement of peripheral olfactory projections. Science 304, 1976-1979.

Accepted December 12, 2005